Macromolecules

Article

pubs.acs.org/Macromolecules

Figure-Eight-Shaped and Cage-Shaped Cyclic Polystyrenes

Taeheon Lee,[†,⊥] Joongsuk Oh,[§,⊥] Jonghwa Jeong,[†] Haeji Jung,[†] June Huh,[*,‡] Taihyun Chang,[*,§] and Hyun-jong Paik[*,†]

[†]Department of Polymer Science and Engineering, Pusan National University, Busan, 46241, Korea

[‡]Department of Chemical and Biological Engineering, Korea University, Seoul, 02841, Korea

[§]Department of Chemistry and Division of Advanced Materials Science, Pohang University of Science and Technology (POSTECH), Pohang, 37673, Korea

Supporting Information

ABSTRACT: Nonlinear polystyrenes (PS) with similar molecular weights but with different molecular structures having star-, figure-8-, and cage-shaped architectures were synthesized by combining atom transfer radical polymerization (ATRP) and click chemistry. Figure-8- and cage-shaped PS were fractionated by using a gradient normal phase liquid chromatography as confirmed by SEC-LS, MALDI–TOF MS, ^{1}H NMR, and FT-IR spectrometry. Their purities were estimated by using a two-dimensional liquid chromatography (2D-LC). The glass transition temperatures of these topologically different polymers were in the order of cage-, figure-8-, and star-shaped polymers possibly due to the multiple links that constrain the overall molecular diffusivity in the case of multicyclic polymers (figure-8, and cage). Monte Carlo simulation on the glass transition behavior of model system also agreed well with the experimental results.

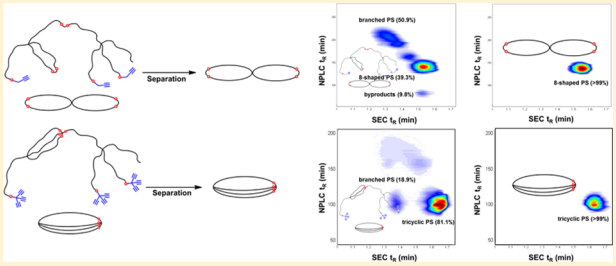

1. INTRODUCTION

Topological control of polymers has provided new opportunities in polymer science since it gives unprecedented properties originated from nonlinear molecular architectures such as star-like,[1] comb-like,[2] dendrimer,[3] and cyclic polymers.[4] Among various architectural topologies of polymers, cyclic polymers have attracted significant attention due to their unique properties associated with chain topologies.[5−8] Recently, the synthesis of multicyclic polymers has been reported vigorously with the demand for new polymer materials from polymer application fields. For example, the Tezuka group has pioneered synthesis of different topological multicyclic poly(THF)s, including fused,[6,7] spiro,[9] and bridged forms,[10] using electrostatic self-assembly and covalent fixation under dilute condition. Numerous researchers have endeavored to prepare various topologically appealing multicyclic polymers including sun-shaped,[11,12] tadpole-shaped,[13−17] 8-shaped,[18,19] manacle-shaped,[20] and paddle-shaped polymers[21] through controlled radical polymerization or anionic polymerization. Their complex molecular topologies involving cycles in various fashions offer a new opportunity to tune thermomechanical and dynamical properties without changing chemical species of the materials. For instance, the molecular topological constraints such as internal cross-links and physical knots can result in nontrivial effects on the molecular diffusivity and the glass transition temperature. However, very few works have been conducted for the structure–property correlations of cyclic polymers due to the difficulty in preparing those molecules with high purity.[8,22]

We recently reported the preparation of bicyclic polystyrene (PS) by using combination of ATRP and "click" chemistry[23,24] efficient strategy for cyclization based on first report from Grayson group.[25] In our precious reports, the 3-arm star PS was synthesized by ATRP and used it as a precursor polymer for bicyclic polymer after simple azidation of 3-arm star polymer. ATRP techniques provide halogen terminal convertible into versatile chain-end functionality such as azido-functionality clickable with alkyne-functionality.[26] However, there is inherent difficulty to preserve the chain-end functionality since ATRP is not truly a living process.[27] Because of imperfect chain-end functionality of precursor polymer and linking reaction of several polymer for multifunctional coupling agent, this system produces high-molecular-weight impurities along with bicyclic polymer. Therefore, it is necessary to fractionate the target bicyclic polymer from the byproducts.

In this paper, we report the synthesis of two topologically different multicyclic polymers, namely, figure-8-shaped (8-cyc) and cage-shaped (C-cyc) polymers (Scheme 1), and compare their glass transition behavior in terms of chain topological effect. The 8- and C-cyc polymers were successfully synthesized by combining atom transfer radical polymerization (ATRP) and "click" chemistry with difunctional and tetrafunctional coupling agents, and purified by fractionation with a gradient normal phase liquid chromatography (NPLC). Their purities were

Received: January 14, 2016
Revised: April 22, 2016

DOI: 10.1021/acs.macromol.6b00093
Macromolecules XXXX, XXX, XXX–XXX

Scheme 1. Overall Scheme for Synthesis of 8-cyc and C-cyc Polymers[a]

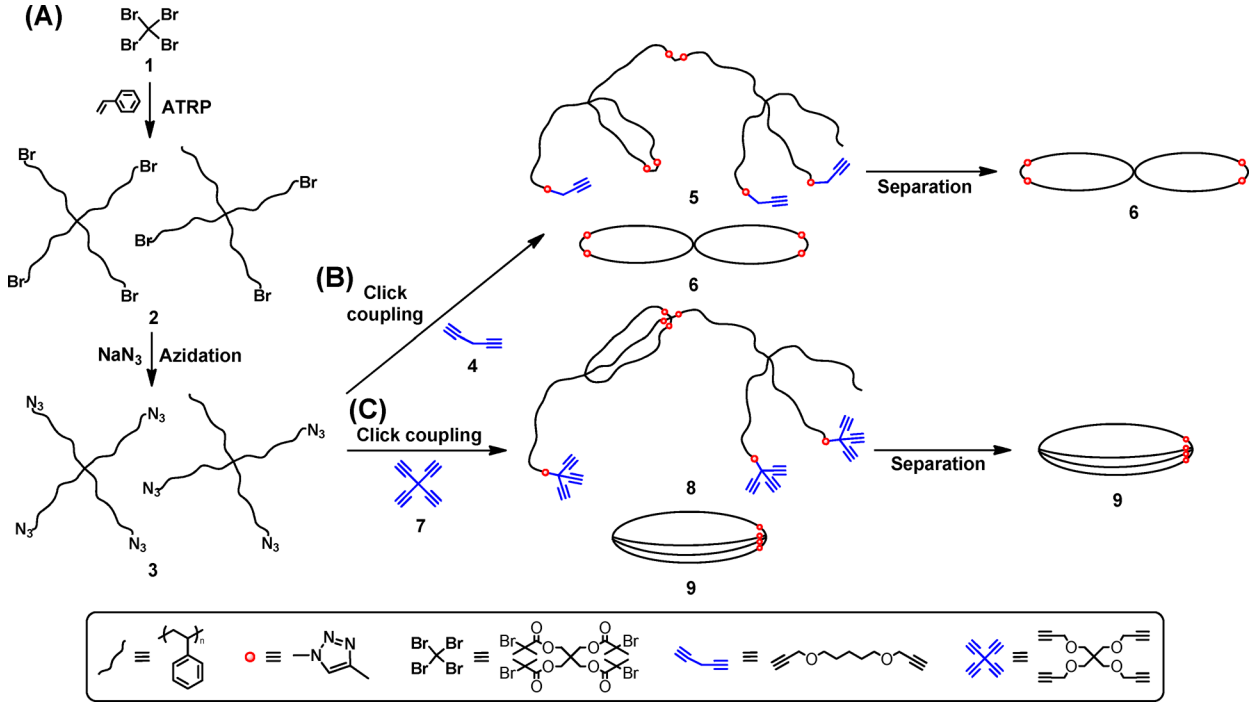

[a]Key: (A)Synthesis of 4-arm star polymer by ATRP from tetra-functional initiator, (B) synthesis of 8-cyc PS (**6**) between 4-arm star polymer and di-functional coupling agent by "click" chemistry, and (C) synthesis of C-cyc PS (**9**) between 4-arm star polymer and di-functional coupling agent by "click" chemistry.

examined by using two-dimensional liquid chromatography (2D-LC). The glass transition behavior of these high-purity multicyclic polymers was investigated by differential scanning calorimetry (DSC) and compared with Monte Carlo simulation of model cyclic chain systems.

2. METHODS

Materials. Styrene (Junsei, 99.5%) was purified before use by passage through and alumina column to remove the inhibitor and stabilizer. Copper(I) bromide (CuBr, Aldrich, 98.0%) was purified by stirring with glacial acetic acid, followed by filtering and washing the solid four times with ethanol and twice with diethyl ether. The solid was dried under vacuum for 2 days. Tetrahydrofuran (THF, J. T. Baker, 100%) was distilled over CaH_2. *N,N,N′,N″,N″*-Pentamethyldiethylenetriamine (PMDETA, 98%), pentaeryethritol (99.0%), 1,5-dipentanediol (96.0%), triethylamine (TEA, 99.5%), copper(II) bromide ($CuBr_2$, 98.0%), 2-bromoisobutyryl bromide (98.0%), dithranol (90%), and NaTFA (98%) were purchased from Aldrich and used as received. Magnesium sulfate ($MgSO_4$, Junsei), propargyl bromide (TCI), sodium azide (NaN_3, Junsei) and all other chemicals were used as received.

Instruments. For size exclusion chromatography (SEC) analysis, three PS/DVB columns (Agilent Polypore 300 × 7.5 mm, Waters Styragel HR4 300 × 7.8 mm, and Jordi mixed bed 300 × 8.0 mm) were used. A Viscotek TDA302 detector was used for differential refractometry (RI) and light scattering (LS) detection. Eluent was THF delivered by a Bischoff HPLC compact pump at a flow rate of 0.7 mL/min. For 2D-LC analysis, the two LC systems were connected by an electronically controlled 2-position, 10 port switching valve (Alltech, SelecPro). The first dimension of 2D-LC was solvent gradient normal phase liquid chromatography (NPLC) and the second dimension was SEC. In the first-D LC, a bare silica column (Nucleosil, 5 μm, 100 Å pore, 150 × 4.6 mm) was used and THF/*n*-hexane mixture was used as the eluent. Flow rate of the first-D LC was set at 0.05 mL/min to synchronize with the second-D SEC separation. The solvent gradient program for the first LC separation was set as follows (solvent A, THF/*n*-hexane = 40/60; solvent B, THF/*n*-hexane = 60/40), The eluent was kept at A for the first 100 min then the eluent was changed from A to B linearly for the next 200 min. In the second LC, a polypore mixed bed column (Agilent, 5 μm, 250 × 4.6 mm) was used for SEC separation and THF was used as the eluent. Flow rate of the second-D SEC was set at 1.6 mL/min for a fast analysis. Temperature of the second-D SEC column was controlled at 70 °C by a column oven (Futecs, AT-4000). NPLC- setup for the purification of the as-prepared sample was the same as the first dimension NPLC of the 2D-LC analysis except for the flow rate and the solvent gradient program. Flow rate was set at 0.5 mL/min and the eluent was kept at A for the first 30 min then changed linearly to B during the next 30 min. Monomer conversion was determined by HP 5890 gas chromatography equipped with HP101 column (methyl silicone fluid, 25 m × 0.32 mm × 0.30 μm). ^{1}H NMR spectra were obtained on a Varian Unity Inova 500 MHz superconducting FT-NMR spectrometer using $CDCl_3$ as solvent. Infrared spectra were recorded on a Nicole 6700 FT-IR spectrophotometer. Differential scanning calorimeter (DSC) analyses were performed with TA Instruments Q 100, which operated at 10 °C/min under nitrogen gas. A Bruker Autoflex speed mass spectrometer equipped with a 2k Hz smartbeam-II laser was used for MALDI−TOF MS experiments. The instrument operated at an accelerating potential of 20 kV in positive mode. Mass calibration was performed using homemade PS standards. Dithranol and DCTB were used as MALDI matrix. NaTFA were used as cationization agent. They were dissolved in THF and a small aliquot was deposited on a MALDI plate.

Synthesis of Pentaerythritol Tetrakis(2-bromoisobutyrate) (1). Pentaerythritol (4.0 g, 29.4 mmol) was added to the N_2 purged round-bottom flask with 100 mL of dried THF and then TEA (19.7 mL, 141 mmol) added to the flask. 2-Bromoisobutyryl bromide (17.4 mL, 141 mmol) was injected dropwise to the above flask at 0 °C over 30 min. The reaction mixture was reacted at room temperature for the next 12 h. After reaction, reaction mixture was washed with H_2O/diethyl ether. The organic phase was dried over $MgSO_4$. Diethyl ether was removed using a rotary evaporator. The product was recrystallized in hexane. Thus 12.25 g of the white crystalline product was obtained (yield: 57%). ^{1}H NMR (400 MHz, $CDCl_3$): δ = 4.33 (s, 8H), 1.94 (s, 24H).

DOI: 10.1021/acs.macromol.6b00093
Macromolecules XXXX, XXX, XXX−XXX

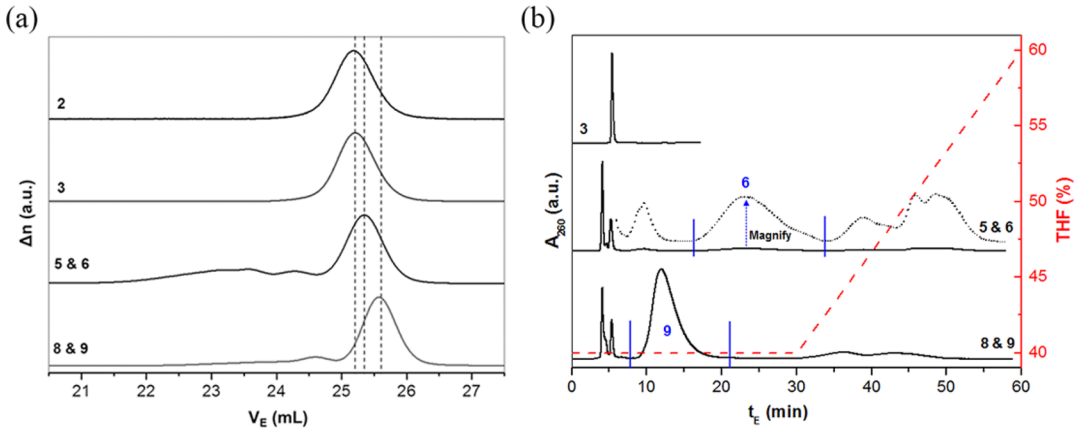

Figure 1. (a) SEC-LS traces of **2**, **3**, as-synthesized 8-cyc PS (mixture of **5** and **6**), as-synthesized C-cyc PS (mixture of **8** and **9**) and (b) solvent gradient NPLC chromatograms of 4-arm star precursor (**3**), as-synthesized 8-cyc PS (mixture of **5** and **6**), and as-synthesized C-cyc PS (mixture of **8** and **9**).

*Synthesis of 1,5-Bis(2-propynyloxy)pentane (**4**).* Sodium hydride (NaH, 1.04 g, 43.2 mmol) was added to the round-bottom flask containing a solution of 1,5-pentanediol (1.5 g, 14.4 mmol) in DMF (50 mL). Propargyl bromide (3.85 mL, 43.2 mmol) was added slowly to the flask with stirring at 0 °C. After addition of propargyl bromide, the reaction was carried out at 60 °C for 24 h. The reaction mixture was extracted with ethyl acetate followed by washing with deionized water several times. The organic phase was dried over $MgSO_4$ and the volatiles were removed in vacuo. The crude product was further purified by column chromatography using hexane/ethyl acetate (3/1). After drying, 1.68 g of the brown oil was obtained in 65% yield. ^{1}H NMR ($CDCl_3$): δ = 4.13 (s, 4H), 3.52 (s, 4H), 2.40 (s, 2H), 1.63 (s, 4H), 1.44 (s, 2H).

*Synthesis of Tetrakis(2-propynyloxymethyl)methane (**7**).* NaH (1.06 g, 44.1 mmol) was added to the round-bottom flask containing a solution of pentaerythritol (1.0 g, 7.34 mmol) in DMF (100 mL). Propargyl bromide (3.93 mL, 44.1 mmol) was added slowly to the reaction vessel with stirring at 0 °C. After addition of propargyl bromide, the reaction was carried out at 60 °C for 24 h. The reaction mixture was extracted with ethyl acetate followed by washing with deionized water several times. The organic phase was dried over $MgSO_4$ and the volatiles were removed in vacuo. The crude product was further purified by column chromatography using hexane/ethyl acetate (3/1). After drying, 1.24 g of the brown oil was obtained in 60% yield. ^{1}H NMR (400 MHz, $CDCl_3$): δ = 4.12 (s, 8H), 3.53 (s, 8H), 2.40 (s, 4H).

*Synthesis of 4-Arm Star Polystyrene (**2**).* CuBr (47 mg, 0.33 mmol), $CuBr_2$ (7.31 mg, 0.03 mmol), PMDETA (0.752 mL, 0.36 mmol) and pentaerythritol tetra(2-bromoisobutyrate) (206 mg, 0.36 mmol) were added to a dried 100 mL Schlenk flask. The flask was sealed with glass stopper then evacuated and backfilled with N_2 three times. Deoxygenated styrene (20 mL, 175 mmol) and anisole (5 mL) were added to the flask via syringes. Then, the flask was placed in an oil bath at 100 °C. At 20% monomer conversion (measured by gas chromatography), the polymerization was quenched by exposing to air. The reaction mixture was diluted with THF and passed through a neutral alumina column to remove the copper catalyst. The polymer was obtained by precipitation in methanol. The polymer was collected by filtration and dried under vacuum. The molecular weight of the obtained polymer was determined by SEC-LS (M_w = 6700 and M_w/M_n = 1.05).

*Synthesis of Azido-Terminated 4-Arm Star Polystyrene (**3**).* Sodium azide (97.3 mg, 1.50 mmol) was added to a solution of **2** (2 g, 0.54 mmol) in DMF (10 mL). The reaction was conducted at room temperature for 24 h. The reaction mixture was diluted with chloroform and washed with deionized water several times. The organic phase was dried with $MgSO_4$. After filtration of solid, solvent was evaporated. The polymer was obtained by precipitation in methanol. The polymer was collected by filtration and dried under vacuum. The molecular weight of the obtained polymer was measured by SEC-LS (M_n = 6700 and M_w/M_n = 1.05). The chain-end functionality of **3** was determined by ^{1}H NMR (chain-end functionality =92%).

*Synthesis of Figure-8-Shaped (8-cyc) PS (**6**).* CuBr (3.10 g, 21.6 mmol) was added to a Schlenk flask, which was subsequently evacuated and backfilled with N_2 three times. Deoxygenated PMDETA (4.51 mL, 21.6 mmol) and THF (200 mL) were added to the flask via syringes. **3** (0.5 g, 0.06 mmol) and **4** (33.4 mg, 0.19 mol) put in 20 mL of THF and were degassed, respectively. Then, those solutions were added dropwise to the solution of CuBr/PMDETA at 35 °C using a syringe pump at the rate of 0.2 mL/h. After complete addition, the reaction was allowed to proceed at 35 °C for 5 h. The reaction mixture was passed through a neutral alumina column to remove the copper catalyst. THF was removed using a rotary evaporator. Pure **6** was separated from its mixture with branched PS (**5**) using a gradient NPLC (M_w = 6700 and M_w/M_n = 1.02).

*Synthesis of Cage-Shaped (C-cyc) PS (**9**).* CuBr (3.10 g, 21.6 mmol) was added to a Schlenk flask, which was subsequently evacuated and backfilled with N_2 three times. Deoxygenated PMDETA (4.51 mL, 21.6 mmol) and THF (200 mL) were added to the flask via syringes. **3** (0.5 g, 0.06 mmol) and **7** (26.7 mg, 0.09 mmol) put in 20 mL of THF and were degassed, respectively. Then, those solutions were added dropwise into the solution of CuBr/PMDETA at 35 °C using a syringe pump at the rate of 0.2 mL/h. After complete addition, the reaction was allowed to proceed at 35 °C for 5h. The reaction mixture was passed through a neutral alumina column to remove the copper catalyst. THF was removed using a rotary evaporator. Pure **9** was separated from its mixture with branched PS (**8**) using a gradient NPLC (M_w = 6700 and M_w/M_n = 1.01).

Monte Carlo Simulation. Dynamic Metropolis Monte Carlo method with the 8-site bond fluctuation model[28,29] is used to investigate the glass transition behavior of star, 8-cyc and C-cyc polymers. Topologically monodisperse chains, each of which has a given architecture with a fixed number of 36 bonds, were generated on a $L \times L \times L$ simulation box with $L = 100a$ under the periodic boundary condition where a is the unit lattice spacing. In order to model the glassy behavior of polymer chain, we employ the potential proposed by Wittkop et al.[30,31] without nonbonded potential for isolating chain architecture effect. The bonded potential $U_b(\mathbf{r})$ was given as

$$U_b(\mathbf{r}) = \begin{cases} 4.461\epsilon & \text{for } \mathbf{r} = (\pm 2, 0, 0) \\ 2.201\epsilon & \text{for } \mathbf{r} = (\pm 2, \pm 1, 0) \\ -0.504\epsilon & \text{for } \mathbf{r} = (\pm 3, 0, 0) \\ -3.275\epsilon & \text{for } \mathbf{r} = (\pm 3, 0, 0) \\ -3.478\epsilon & \text{for } \mathbf{r} = (\pm 2, \pm 2, \pm 1) \\ -1.707\epsilon & \text{for } \mathbf{r} = (\pm 3, \pm 1, 0) \end{cases} \quad (1)$$

DOI: 10.1021/acs.macromol.6b00093
Macromolecules XXXX, XXX, XXX−XXX

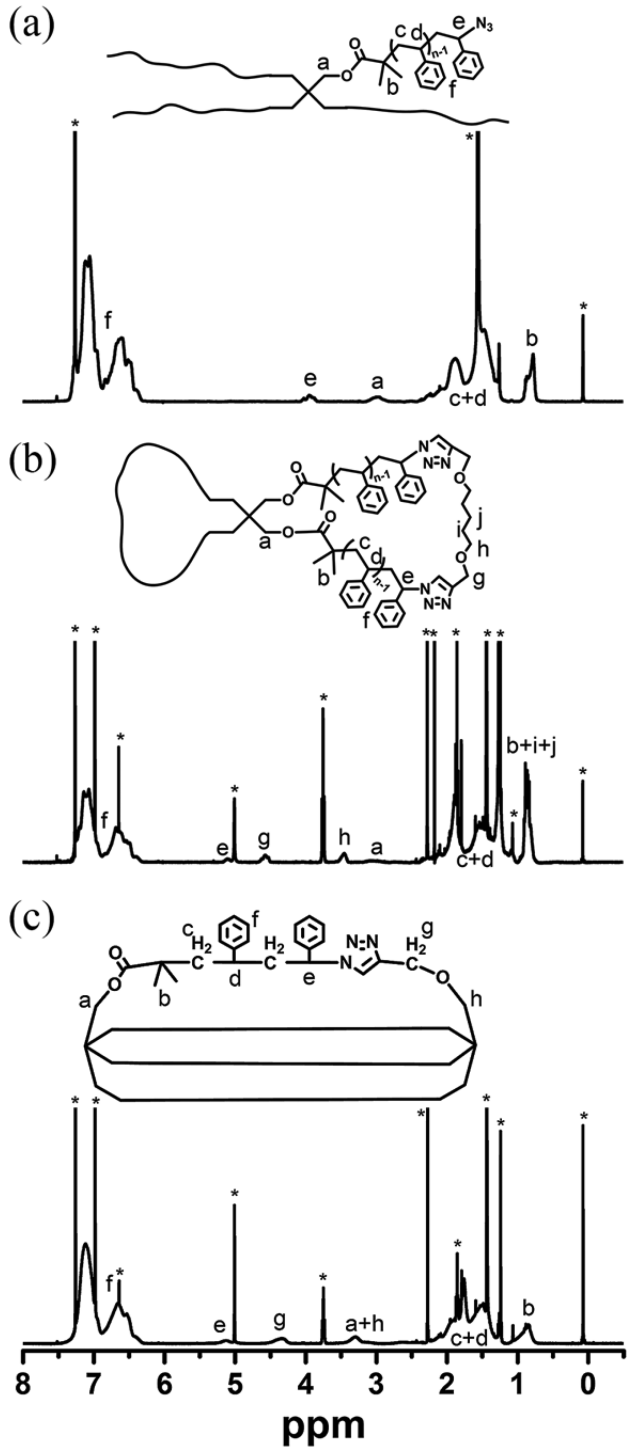

Figure 2. ^{1}H NMR spectra of **3**, **6**, and **9**.

where **r** = (*x*,*y*,*z*) represent the set of all permutations of eigen values of the bond vector in the bond fluctuation model and ε is the unit of energy. A lattice occupation density is set to be $\phi = 0.5$ for polymer chains in the simulation box, which corresponds to a polymer melt in the bond fluctuation model.[32] Each system of randomly generated configuration was initially equilibrated at $k_BT/\varepsilon = \infty$ for 1×10^6 Monte Carlo steps. (MCS) and then annealed at a given k_BT/ε for 2×10^7 MCS.

3. RESULTS AND DISCUSSION

The 4-arm star PS (**2**) was synthesized by ATRP using the tetrafunctional initiator, pentaerythritol tetrakis(2-bromoisobutyrate) (**1**), of which the chemical structure was characterized in

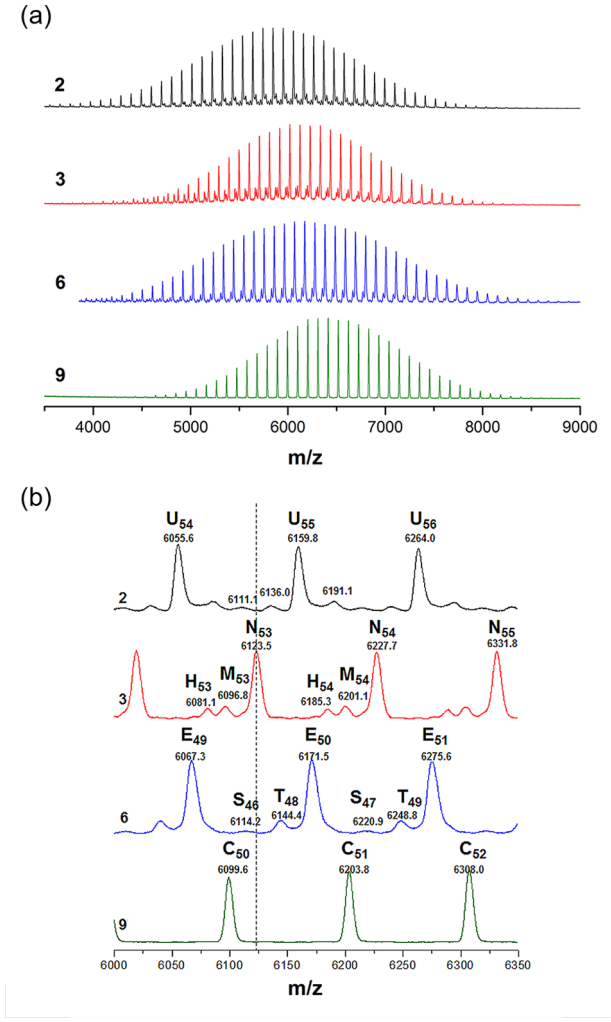

Figure 3. MALDI−TOF MS spectra of **2**, **3**, **6**, and **9**: (a) overall spectra and (b) expanded spectra of near the maxima of peak envelopes.

Figure S1. The bromo chain-end functionality of **2** was determined as ~92% by comparing the methyl protons (0.97−0.70 ppm) at the initiator part to methine proton (4.59−4.36 ppm) adjacent to the terminal bromide group in the ^{1}H NMR spectrum. The bromo chain-end groups of **2** were quantitatively transformed to azido groups by simple nucleophilic substitution reaction as shown in the ^{1}H NMR spectrum (Figure S2). The azido-transformation in the precursor polymer (**3**) was also characterized by the appearance of peak due to azide group at 2100 cm^{-1} in the FT IR spectrum (Figure S3). Di- (**4**) and tetra- (**7**) alkynyl coupling agents were synthesized using propagyl bromide (Figures S4 and S5).

8-cyc (**6**) and C-cyc (**9**) PS were prepared by a "click" coupling reaction between **3** and coupling agents, **4** or **7** respectively, under a dilute condition (2.5 g/L) to minimize the intermolecular coupling reaction resulting in branched high-molecular-weight polymers. The multicyclic polymer (**6** or **9**) was formed along with branched polymers (**5** or **8**, respectively), as evidenced by SEC (Figure 1a). As shown in Figure 1a, **2** (25.19 min) and **3** (25.21 min) are not much different since azidation does not change the topology. However, cyclization of **3** changed the elution time of the multicyclic polymers, **6** (25.4 min) and **9** (25.6 min). The relative delay in the elution of multicyclic polymers, **6** and **9** is due to their reduced hydrodynamic volume. The larger shift for **9** than **6** indicates that

DOI: 10.1021/acs.macromol.6b00093
Macromolecules XXXX, XXX, XXX−XXX

Table 1. Symbol, Structure, and Relative Mass Difference (m/z) Values of the Peaks Observed in MALDI−TOF Mass Spectra

symbol of peak series	description	structure	relative m/z difference from N	symbol in Scheme 1
U	4-arm star PS with 4-terminal double bonds	I−(PS)$_{n-4}$−(C$_8$H$_7$)$_4$	−172 (+36)	2
N	4-arm star PS with 4-terminal azide groups	I−(PS)$_n$−(N$_3$)$_4$	0	3
M	metastable peak of N	I−(PS)$_n$−(N$_3$)$_3$−(N)	−25−27	3
H	4-arm star PS with 3-terminal azide groups	I−(PS)$_n$−(N$_3$)$_3$−H	−41	3
E	8-cyc PS	I−(PS)$_n$−(2N$_3$−**4**)$_2$	+360 (+48)	6
T	tadpole-shaped PS	I−(PS)$_n$−(2N$_3$−**4**)−(N$_3$−4)$_2$	+540 (+20)	6
S	4-arm star PS with 4-terminal triazole ring	I−(PS)$_n$−(N$_3$−**4**)$_4$	+720 (−8)	6
C	C-cyc PS	I−(PS)$_n$−(4N$_3$−7)	+288 (−24)	9

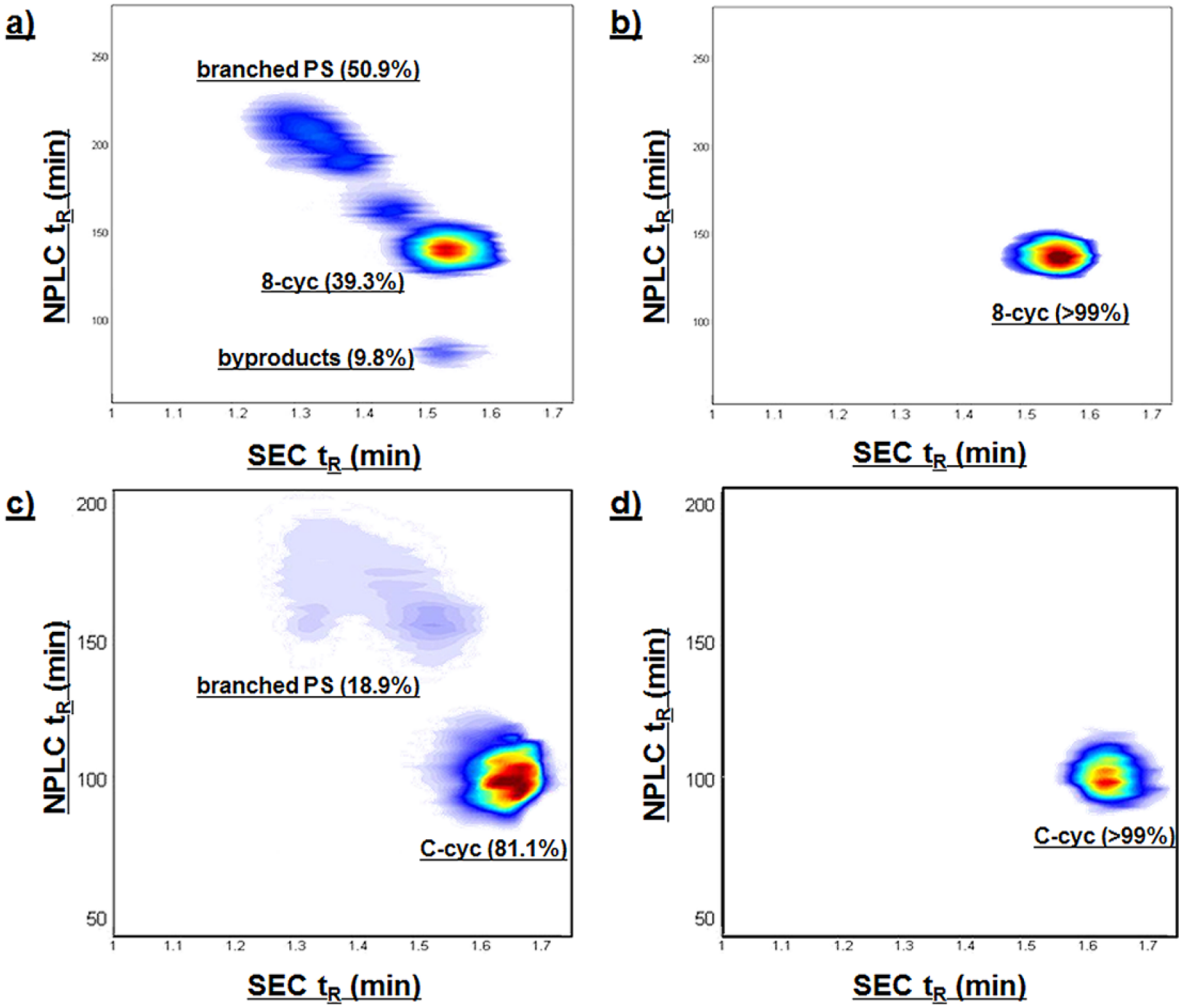

Figure 4. 2D contour plots of (a) mixture of **5** and **6**, (b) **6**, (c) mixture of **8** and **9**, and (d) **9**: the first D, NPLC; the second D, SEC.

the shrinkage of the chain size is larger for **9** than **6**. The appearance of broad multimodal peaks (21.5−24.7 min) on SEC trace of a mixture of **5** and **6** indicates the formation of complex branched byproducts along with **6**. **3** has 90% of azido-functionality predicted by ^{1}H NMR spectroscopy (Figure S2). Thus, lacked precursor polymer must produce byproducts; on coupling with alkynyl groups of **4** produced **5** which could have reactive acetylene groups. These acetylene groups could react further with precursor polymers resulting in the formation of dimeric or multimeric branched high-molecular-weight polymers. Similarly, the mixture of **8** and **9** also showed broad multimodal peaks after click reaction between **3** and **7**. To remove high-molecular-weight branched polymer, cyclic polymers were separated from both mixtures of **5** and **6** and of **8** and **9** respectively, by fractionation with gradient NPLC as shown in Figure 1b. While **3** eluted as a sharp single peak at $V_E \sim 5$ min, for **5** and **6** and for **8** and **9** they elute over a wide elution time (t_E) indicating that they contain a number of byproducts. The main peaks labeled as **6** and **9** in Figure 1b are the elution peaks of the target products, 8-cyc PS and C-cyc PS, respectively. **9** eluted earlier than **6** despite the identical molecular weight due to the different architectures that affects the interaction of polymer chains with the stationary phase differently. To obtain the high purity cyclic polymers, they are fractionated by collecting the effluents over the t_E between the small vertical bars shown in the Figure 1b.

Figure 2 shows the ^{1}H NMR spectra of **3** and separated cyclic polymers, **6** and **9**, from each mixture. As a result of

DOI: 10.1021/acs.macromol.6b00093
Macromolecules XXXX, XXX, XXX−XXX

"click" coupling reaction, the methine proton at 3.98 ppm in the N_3-terminated star polymer (Figure 2a) appeared at 5.12 ppm due to the neighboring triazole unit in the cyclic polymer (Figure 2, parts b and c). Also a new peak at 4.35 ppm appears for the methylene protons in the linker adjacent to the triazole unit.

Figure 3 shows the results of MALDI−TOF MS analyses of the synthesized polymers. In Figure 3a, the overall MALDI−MS peak envelops of precursors and cyclic polymers show nearly the same molecular weight distribution centered around 6.0k in agreement with the molecular weight determined by SEC-LS and ^{1}H NMR. Additionally, expanded spectra of near the maxima of peak envelope were analyzed in Figure 3b. For **2**, the major peak series is U (see Table 1) and they were formed upon elimination of HBr during the MALDI process leaving a double bond at the terminal styrene unit. It is also well-known that a few subsidiary peaks can show up depending on the sample preparation and MALDI process due to the reaction of terminal Br.[33] The spectrum of **3** shows major peak designated as N (target structure with 4 azide groups) and some minor peaks. H seems to be the species having one less azide group. It is likely to have been formed when an arm is terminated during the ATRP. M is the metastable species (−26 m/z) that is always observed for the azido-functionalized polymers.[34] For **6**, some byproduct species are still found in addition to the main target 8-cyc (E series). T and S series can be assigned to the tadpole shaped (a ring with two tails) and 4-arm star PS with 4-terminal triazole rings. The m/z value of E series for 50mer was found to be 6171.5 in excellent agreement with the calculated value (m/z_{cal}.: 6171.7, $C_{443}H_{464}O_{12}N_{12}Na^+$) indicating that the target 8-cyc PS was synthesized successfully. However, the 8-cyc PS was not fractionated perfectly by HPLC since the byproducts elute very close to the major peak as shown in Figure 1b. On the other hand, the MALDI MS spectrum of **9** appears to be very pure as expected from the well-isolated HPLC peak in Figure 1b. In addition, the m/z value of **9** was measured as 6099.5 that is in good agreement with the calculated m/z value of 6099.6 for 50mer ($C_{438}H_{452}O_{12}N_{12}Na^+$).

2D-LC was carried out to assess the purity of **6** and **9**. Figure 4a and 4c show the 2D-LC chromatograms of **5** and **6** and of **8** and **9**, respectively, before the NPLC fractionation. After the click reaction, the presence of the large amount of byproduct is apparent. The purity of **6** is only 39% poorer than **9** (81%). It seems to be a natural result since the probability of making **6** requires two linkers to react with a 4-arm star together while **9** requires only one linker to react with a 4-arm star. After the purification by NPLC fractionation (Figure 2b), most of the byproducts disappeared. The small amount of seemingly tadpole-shaped byproduct in 8-cyc PS observed in MALDI−MS (T series) was not detected in 2D-LC indicating that it elutes very close to **6**.

After fractionation of **3**, **6**, and **9** using the NPLC, an isolated effect of chain topology on thermal behavior was investigated. Figure 5 shows the DSC curves of **3**, **6** and **9**. The glass transition temperatures of these topologically different PSs are in the order of **9** (C-cyc, T_g = 114.5 °C), **6** (8-cyc, T_g = 83.9 °C), and **3** (4-arm star, T_g = 80.8 °C). This glass transition behavior is reflective of more severe topological constraints for molecular motion in **9** (C-cyc polymer) that contains two focal points, as compared to **6** (8-cyc) and **3** (star polymer) having a single focal point. It can be also inferred that higher T_g of **6** in comparison with that of **3** is attributed to the architectural

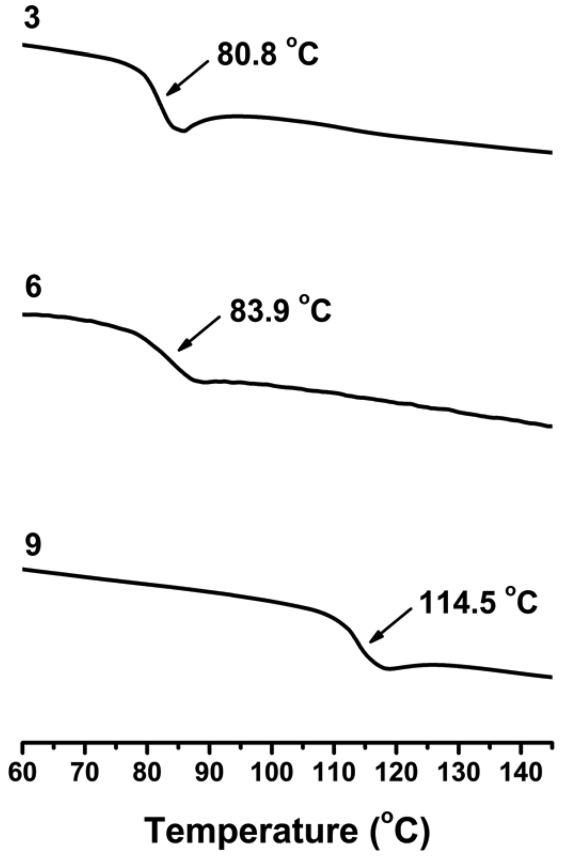

Figure 5. Glass transition temperatures for **3** (a), **6** (b), and **9** (c).

characteristics of 8-cyc polymer where the chain termini are absent.

In order to further investigate the chain architecture effect on the glass transition temperature, we simulated model bulk systems of star, 8-cyc, and C-cyc polymers by employing a dynamic Monte Carlo method with bond fluctuation model. The glass transition of the model chain is reflected by introducing the bonded potential eq 1 that energetically favors a certain bond vector. In the model systems (star, 8-cyc, and C-cyc), the number of bonds per chain is kept constant so as to isolate the architecture effect on the glass transition behavior. The detail of simulation method is described in the Simulation section. For the determination of the glass transition temperature, we used the Vogel−Fulcher relation given by[35−37]

$$D(T) = D_\infty \exp[-A/(T - T_o)] \quad (2)$$

where $D(T)$ is the self-diffusion constant at a temperature T and the D_∞, A, and T_0 are the fit parameters for Vogel−Fulcher relation. Here the T_0, referred to as Vogel−Fulcher temperature, can be interpreted as a thermodynamic limit of glass transition temperature where the relaxation time of polymer becomes infinity. In the present work, the glass transition behavior of star, 8-cyc, and C-cyc is investigated in terms of the Vogel−Fulcher temperature T_0. The self-diffusion constants were estimated from the mean-square displacement $g_1(t)$ of the chain segments as a function of time t:

$$g_1(t) = \langle [\mathbf{R}_s(t) - \mathbf{R}_s(0)]^2 \rangle \quad (3)$$

where $\mathbf{R}_s(t)$ is the position vector of segment at time t and the bracket $\langle\ \rangle$ stands for the average over all segments in

DOI: 10.1021/acs.macromol.6b00093
Macromolecules XXXX, XXX, XXX−XXX

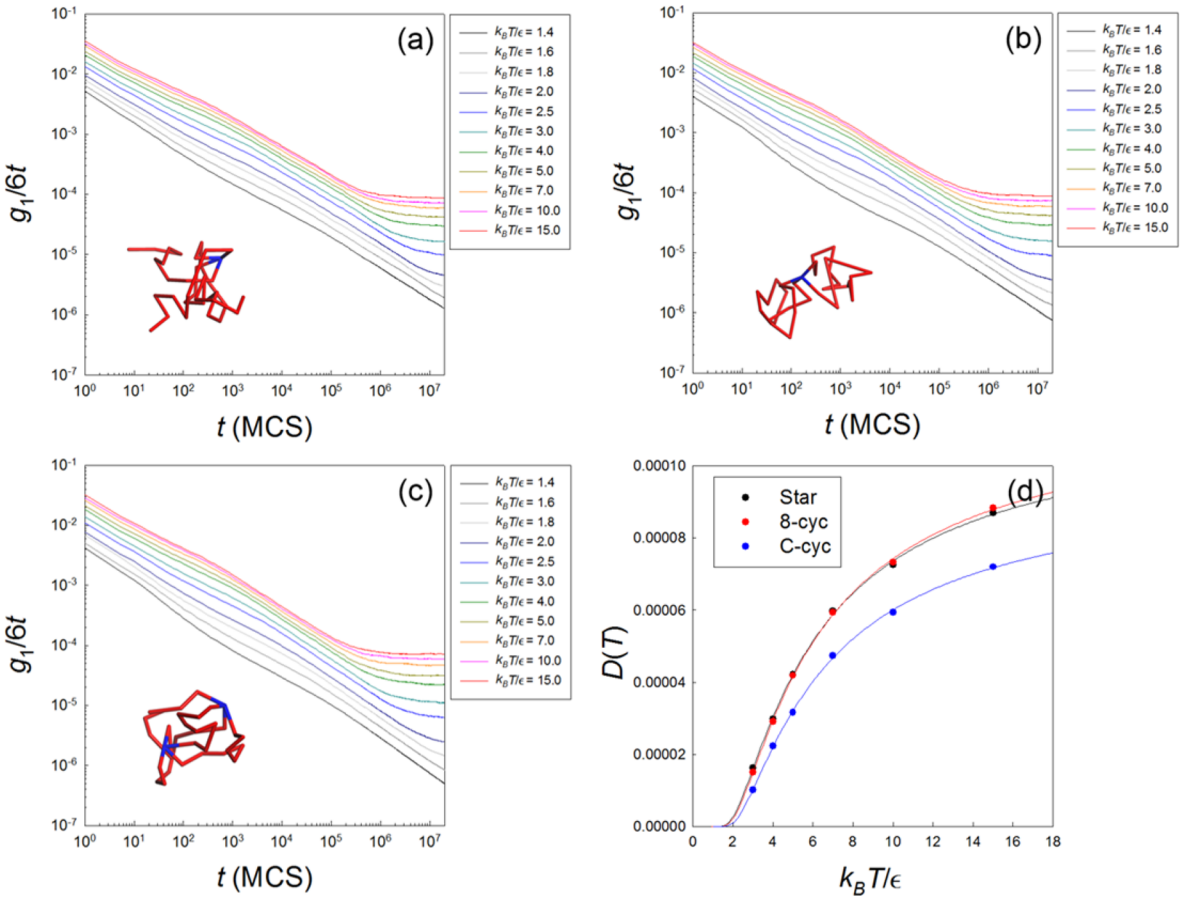

Figure 6. (a–c) Double logarithmic plots of $g_1/6t$ vs t for the simulated systems for (a) star, (b) 8-cyc, and (c) C-cyc. (d) Self-diffusion constants for star, 8-cyc, and C-cyc as a function of temperature.

the simulated system. Since the mean square displacement should show a diffusive behavior, $g_1(t) = 6Dt$, at $t > \tau$ where τ is the relaxation time of the chain, we can estimate the self-diffusion constant D from a plateau in the plot of g_1/t vs t.

Figure 6 presents double logarithmic plots of $g_1/6t$ vs t for the simulated systems for **3** (Figure 6a), **6** (Figure 6b) and **9** (Figure 6c), respectively. The $g_1/6t$ curves for **3**, **6**, and **9** show well-defined plateau regimes at $\tilde{T}(=k_BT/\varepsilon) = 3.0–15.0$ after sufficiently long time simulations ($\sim O$ (10^6) MCS), whereas no clear plateaus (or crossover to the diffusive regime) were yet reached at $\tilde{T} < 2.5$ even after 2×10^7 MCS. Figure 6d shows the self-diffusion constants for **3**, **6**, and **9** as a function of $\tilde{T}$ estimated from Figure 6a-6c. The solid lines represent Vogel–Fulcher fits eq 2 with three adjustable parameters including Vogel–Fulcher temperature, which give $D_\infty = 0.000116$, $A = 4.165$, and $\tilde{T}_o = 0.900$ for star, $D_\infty = 0.000119$, $A = 4.290$, and $\tilde{T}_o = 0.933$ for 8-cyc, and $D_\infty = 0.000099$, $A = 4.452$, and $\tilde{T}_o = 1.034$ for C-cyc, respectively. The Vogel–Fulcher analysis reveals that $\tilde{T}_o$ for **9** is higher than $\tilde{T}_o$ for **3** and **6**, which is reflective of more restrictive bond constraints for **9**, as also manifested by smaller self-diffusion constant for **9**. It is also found from the simulation that $\tilde{T}_o$ of **6** is nearly the same with $\tilde{T}_o$ of **3** although $\tilde{T}_o$ of **6** is slightly higher. The simulation results for three different chain architectures showed that the difference in T_gs between star and 8-shape is much smaller than that between 8-shape and cage-shape, which is also in agreement with the experimental results. The diffusion of the overall polymers with these three architectures, which have commonly 4 bond linked focal point, is governed by the motion of focal point that is the slowest segmental motion. The C-cyc polymers that has two focal points needs more thermal energy preventing the vitrification than star and 8-Cyc polymers, both of which have only one focal point. Given that the slowest motion of such focal point predominantly determine the diffusivity of the overall chain, the glass transition behavior of 8-Cyc is nearly the same as that of star whose dynamics is only slightly enhanced by the local motion of four chain ends.

4. CONCLUSION

In this paper, we describe the synthesis of figure-8-shaped and cage-shaped PSs by combining ATRP and "click" coupling reaction. The structures of figure-8-shaped and cage-shaped PS separated from branched high-molecular-weight polymer byproducts were characterized by SEC, FT-IR, ^{1}H NMR, and MALDI–TOF. Their purities were estimated from 2D-LC analysis. Glass transition temperatures of 4-arm star polymer, figure-8-shaped, and cage-shaped polymer were measured by DSC. T_gs of multicyclic polymers (figure-8-shaped, and cage-shaped polymer) were higher than precursor 4-arm star polymer owing to the topological difference. The observed glass transition behavior also agreed well with the Monte Carlo simulation results based on Vogel–Fulcher analysis.

DOI: 10.1021/acs.macromol.6b00093
Macromolecules XXXX, XXX, XXX–XXX

■ ASSOCIATED CONTENT

Supporting Information

The Supporting Information is available free of charge on the ACS Publications website at DOI: 10.1021/acs.macromol.6b00093.

^{1}H NMR spectra of initiator (**1**), coupling agents (**4**, **7**), star polymers (**2**, **3**) and FT-IR spectra of star polymers (**2**, **3**) and coupling agents (**4**, **7**) (PDF)

■ AUTHOR INFORMATION

Corresponding Authors

*(H.P.) Telephone: +82-51-510-2402. E-mail: hpaik@pusan.ac.kr.
*(T.C.) Telephone: +82-54-279-2109. E-mail: tc@postech.ac.kr.
*(J.H.) Telephone: +82-2-3290-5977. E-mail: junehuh@korea.ac.kr.

Author Contributions

⊥These authors contributed equally to this work

Notes

The authors declare no competing financial interest.

■ ACKNOWLEDGMENTS

This work was supported by the Active Polymer Center for Pattern Integration (No. R11-2007-0056091) and Basic Science Research Program through the National Research Foundation of Korea (NRF) grant funded by the Korean government (MSIP) (2013R1A2A2A01068818). T.C. acknowledges the support from NRF-Korea (2015R1A2A2A01004974). J.H. acknowledges support from NRF-Korea (2013R1A1A2064112).

■ REFERENCES

(1) Schaefgen, J. R.; Flory, P. J. Synthesis of Multichain Polymers and Investigation of their Viscosities. *J. Am. Chem. Soc.* **1948**, *70*, 2709−2718.

(2) Bhattacharya, A.; Misra, B. N. Grafting: A Versatile Means to Modify Polymers: Techniques, Factors and Applications. *Prog. Polym. Sci.* **2004**, *29*, 767−814.

(3) Hawker, C. J.; Frechet, J. M. J. Preparation of Polymers with Controlled Molecular Architecture. A New Convergent Approach to Dendritic Macromolecules. *J. Am. Chem. Soc.* **1990**, *112*, 7638−7647.

(4) Semlyen, J. A. *Introduction: Cyclic Polymers - The First 40 Years. In Cyclic Polymers*; Semlyen, J. A., Ed.; Springer: Dordrecht, The Netherlands, 2002; pp 1−46.

(5) Hadziioannou, G.; Cotts, P. M.; ten Brinke, G.; Han, C. C.; Lutz, P.; Strazielle, C.; Rempp, P.; Kovacs, A. J. Thermodynamic and Hydrodynamic Properties of Dilute Solutions of Cyclic and Linear Polystyrenes. *Macromolecules* **1987**, *20*, 493−497.

(6) Tezuka, Y.; Fujiyama, K. Construction of Polymeric δ-Graph: A Doubly Fused Tricyclic Topology. *J. Am. Chem. Soc.* **2005**, *127*, 6266−6270.

(7) Oike, H.; Imaizumi, H.; Mouri, T.; Yoshioka, Y.; Uchibori, A.; Tezuka, Y. Designing Unusual Polymer Topologies by Electrostatic Self-Assembly and Covalent Fixation. *J. Am. Chem. Soc.* **2000**, *122*, 9592−9599.

(8) Kapnistos, M.; Lang, M.; Vlassopoulos, D.; Pyckhout-Hintzen, W.; Richter, D.; Cho, D.; Chang, T.; Rubinstein, M. Unexpected Power-Law Stress Relaxation of Entangled Ring Polymers. *Nat. Mater.* **2008**, *7*, 997−1002.

(9) Yamamoto, T.; Tezuka, Y. Topological Polymer Chemistry: A Cyclic Approach Toward Novel Polymer Properties and Functions. *Polym. Chem.* **2011**, *2*, 1930−1941.

(10) Sugai, N.; Heguri, H.; Ohta, K.; Meng, Q.; Yamamoto, T.; Tezuka, Y. Effective Click Construction of Bridged- and Spiro-Multicyclic Polymer Topologies with Tailored Cyclic Prepolymers (kyklo-Telechelics). *J. Am. Chem. Soc.* **2010**, *132*, 14790−14802.

(11) Fan, X.; Wang, G.; Huang, J. Synthesis of Macrocyclic Molecular Brushes with Amphiphilic Block Copolymers as Side Cains. *J. Polym. Sci., Part A: Polym. Chem.* **2011**, *49*, 1361−1367.

(12) Liu, L.; Parameswaran, S.; Sharma, A.; Grayson, S. M.; Ashbaugh, H. S.; Rick, S. W. Molecular Dynamics Simulations of Linear and Cyclic Amphiphilic Polymers in Aqueous and Organic Environments. *J. Phys. Chem. B* **2014**, *118*, 6491−6497.

(13) Lord, S. J.; Sheiko, S. S.; LaRue, I.; Lee, H.-I.; Matyjaszewski, K. Tadpole Conformation of Gradient Polymer Brushes. *Macromolecules* **2004**, *37*, 4235−4240.

(14) Wan, X.; Liu, T.; Liu, S. Synthesis of Amphiphilic Tadpole-Shaped Linear-Cyclic Diblock Copolymers via Ring-Opening Polymerization Directly Initiating from Cyclic Precursors and Their Application as Drug Nanocarriers. *Biomacromolecules* **2011**, *12*, 1146−1154.

(15) Doi, Y.; Ohta, Y.; Nakamura, M.; Takano, A.; Takahashi, Y.; Matsushita, Y. Precise Synthesis and Characterization of Tadpole-Shaped Polystyrenes with High Purity. *Macromolecules* **2013**, *46*, 1075−1081.

(16) Oike, H.; Uchibori, A.; Tsuchitani, A.; Kim, H.-K.; Tezuka, Y. Designing Loop and Branch Polymer Topology with Cationic Star Telechelics through Effective Selection of Mono- and Difunctional Counteranions. *Macromolecules* **2004**, *37*, 7595−7601.

(17) Shi, G.-Y.; Tang, X.-Z.; Pan, C.-Y. Tadpole-shaped Amphiphilic Copolymers Prepared via RAFT Polymerization and Click Reaction. *J. Polym. Sci., Part A: Polym. Chem.* **2008**, *46*, 2390−2401.

(18) Schappacher, M.; Deffieux, A. Controlled Synthesis of Bicyclic "Eight-Shaped" Poly(chloroethyl vinyl ether)s. *Macromolecules* **1995**, *28*, 2629−2636.

(19) Fan, X.; Huang, B.; Wang, G.; Huang, J. Synthesis of Amphiphilic Heteroeight-Shaped Polymer Cyclic-[Poly(ethylene oxide)-b-polystyrene]$_2$ via "Click" Chemistry. *Macromolecules* **2012**, *45*, 3779−3786.

(20) Tezuka, Y.; Ohashi, F. Synthesis of Polymeric Topological Isomers through Double Metathesis Condensation with H-Shaped Telechelic Precursors. *Macromol. Rapid Commun.* **2005**, *26*, 608−612.

(21) Lonsdale, D. E.; Monteiro, M. J. Various Polystyrene Topologies Built from Tailored Cyclic Polystyrene via CuAAC Reactions. *Chem. Commun.* **2010**, *46*, 7945−7947.

(22) Hossain, M. D.; Lu, D.; Jia, Z.; Monteiro, M. J. Glass Transition Temperature of Cyclic Stars. *ACS Macro Lett.* **2014**, *3*, 1254−1257.

(23) Jeong, J.; Kim, K.; Lee, R.; Lee, S.; Kim, H.; Jung, H.; Kadir, M. A.; Jang, Y.; Jeon, H. B.; Matyjaszewski, K.; Chang, T.; Paik, H.-j. Preparation and Analysis of Bicyclic Polystyrene. *Macromolecules* **2014**, *47*, 3791−3796.

(24) Jeong, J.; Kim, H.; Lee, S.; Choi, H.; Jeon, H. B.; Paik, H.-j. Improved Synthesis of Bicyclic Polystyrenes by ATRP and "Click" Reaction. *Polymer* **2015**, *72*, 447−452.

(25) Laurent, B. A.; Grayson, S. M. An Efficient Route to Well-Defined Macrocyclic Polymers via "Click" Cyclization. *J. Am. Chem. Soc.* **2006**, *128*, 4238−4239.

(26) Matyjaszewski, K.; Xia, J. Atom Transfer Radical Polymerization. *Chem. Rev.* **2001**, *101*, 2921−2990.

(27) Matyjaszewski, K. Atom Transfer Radical Polymerization (ATRP): Current Status and Future Perspectives. *Macromolecules* **2012**, *45*, 4015−4039.

(28) Carmesin, I.; Kremer, K. Static and Dynamic Properties of Two-Dimensional Polymer Melts. *J. Phys. (Paris)* **1990**, *51*, 915−932.

(29) Deutsch, H. P.; Binder, K. Interdiffusion and Self-Diffusion in Polymer Mixtures: A Monte Carlo Study. *J. Chem. Phys.* **1991**, *94*, 2294−2304.

(30) Wittkop, M.; Hölzl, T.; Kreitmeier, S.; Göritz, D. A Monte Carlo Sudy of The Glass Transition in Three-Dimensional Polymer Melts. *J. Non-Cryst. Solids* **1996**, *201*, 199−210.

(31) Grassberger, P. Pruned-Enriched Rosenbluth Method: Simulations of θ Polymers of Chain Length up to 1 000 000. *Phys. Rev. E: Stat. Phys., Plasmas, Fluids, Relat. Interdiscip. Top.* **1997**, *56*, 3682−3693.

DOI: 10.1021/acs.macromol.6b00093
Macromolecules XXXX, XXX, XXX−XXX

(32) Thompson, R. L.; McDonald, M. T.; Lenthall, J. T.; Hutchings, L. R. Solvent Accelerated Polymer Diffusion in Thin Films. *Macromolecules* **2005**, *38*, 4339−4344.
(33) Kim, K.; Hasneen, A.; Paik, H.-j; Chang, T. MALDI-TOF MS Characterization of Polystyrene Synthesized by ATRP. *Polymer* **2013**, *54*, 6133−6139.
(34) Li, Y.; Hoskins, J. N.; Sreerama, S. G.; Grayson, S. M. MALDI−TOF Mass Spectral Characterization of Polymers Containing an Azide Group: Evidence of Metastable Ions. *Macromolecules* **2010**, *43*, 6225−6228.
(35) Vogel, H. The law of the relationship between viscosity of liquids and the temperature. *Phys. Z.* **1921**, *22*, 645−646.
(36) Fulcher, G. S. Analysis of Recent Measurements of The Viscosity of Glasses. *J. Am. Ceram. Soc.* **1925**, *8*, 339−355.
(37) Okun, K.; Wolfgardt, M.; Baschnagel, J.; Binder, K. Dynamics of Polymer Melts above the Glass Transition: Monte Carlo Studies of the Bond Fluctuation Model. *Macromolecules* **1997**, *30*, 3075−3085.

DOI: 10.1021/acs.macromol.6b00093
Macromolecules XXXX, XXX, XXX−XXX